Characterization of the Structure and Reactivity of Monocopper–Oxygen Complexes Supported by β-Diketiminate and Anilido-Imine Ligands

BENJAMIN F. GHERMAN, WILLIAM B. TOLMAN, CHRISTOPHER J. CRAMER
Department of Chemistry and Supercomputer Institute, University of Minnesota, 207 Pleasant St. SE, Minneapolis, Minnesota 55455

Received 16 March 2006; Revised 24 April 2006; Accepted 25 April 2006
DOI 10.1002/jcc.20502
Published online 3 October 2006 in Wiley InterScience (www.interscience.wiley.com).

Abstract: Copper–oxygen complexes supported by β-diketiminate and anilido-imine ligands have recently been reported (Aboelella et al., J Am Chem Soc 2004, 126, 16896; Reynolds et al., Inorg Chem 2005, 44, 6989) as potential biomimetic models for dopamine β-monooxygenase (DβM) and peptidylglycine α-hydroxylating monooxygenase (PHM). However, in contrast to the enzymatic systems, these complexes fail to exhibit C—H hydroxylation activity (Reynolds et al., Chem Commun 2005, 2014). Quantum chemical characterization of the 1:1 Cu-O_2 model adducts and related species (Cu(III)-hydroperoxide, Cu(III)-oxo, and Cu(III)-hydroxide) indicates that the 1:1 Cu-O_2 adducts are unreactive toward substrates because of the weakness of the O—H bond that would be formed upon hydrogen-atom abstraction. This in turn is ascribed to the 1:1 adducts having both low reduction potentials and basicities. Cu(III)-oxo species on the other hand, determined to be intermediate between Cu(III)-oxo and Cu(II)-oxyl in character, are shown to be far more reactive toward substrates. Based on these results, design strategies for new DβM and PHM biomimetic ligands are proposed: new ligands should be made less electron rich so as to favor end-on dioxygen coordination in the 1:1 Cu-O_2 adducts. Comparison of the relative reactivities of the various copper–oxygen complexes as hydroxylating agents provides support for a Cu(II)-superoxide species as the intermediate responsible for substrate hydroxylation in DβM and PHM, and suggests that a Cu(III)-oxo intermediate would be competent in this process as well.

 J Comput Chem 27: 1950–1961, 2006

Key words: biomimetic copper-oxygen complexes; oxygen activation; C—H bond activation; density functional theory

Introduction

Binding and activation of dioxygen by copper centers plays an important role in the catalytic cycle of an array of enzyme systems.[1,2] Particular examples include the Cu-containing enzymes dopamine β-monooxygenase (DβM)[3,4] and peptidylglycine α-hydroxylating monooxygenase (PHM),[3,5] the former of which hydroxylates the benzylic position of dopamine to yield norepinephrine in the biosynthesis of the neurohormone epinephrine and the latter of which hydroxylates the C_α position of the terminal glycine residue in glycine-extended peptide precursors of neuropeptide hormones. Extensive sequence identity in the two enzymes[6,7] along with conserved active site residues implies that the catalytic mechanisms in DβM and PHM are analogous.[3,8–11] Of the two noncoupled copper centers in these enzymes, Cu_A (or Cu_H) is thought to function as an electron transfer site, while it is Cu_B (or Cu_M) which apparently binds dioxygen and serves as the site of substrate hydroxylation.

Despite significant experimental and theoretical work, definitive identification of the Cu_B-oxygen intermediate that reacts with substrate, the mechanism of Cu_B-oxygen adduct formation, and the mechanism for reaction with substrate remains elusive. Experimental work from Klinman and coworkers[9] on DβM led to the proposal of oxygen binding to copper in a $Cu_B(I)$-O_2/$Cu_B(II)$-O_2^- equilibrium. The Cu(II)-superoxo species functions to abstract a hydrogen atom from substrate, generating a Cu(II)-hydroperoxo species and a substrate free radical. These findings were corrobo-

Correspondence to: C. J. Cramer; e-mail: cramer@chem.umn.edu

Contract/grant sponsor: NIH; contract/grant number: NRSA-GM070144 and GM47365

Contract/grant sponsor: NSF; contract/grant number: CHE-0610183

This article contains Supplementary Material available at http://www.interscience.wiley.com/jpages/0192-8651/suppmat

rated by a crystal structure of a precatalytic complex of PHM obtained via the use of a bound, inactive substrate analog[12] and by theoretical calculations on models of the PHM Cu_B site.[13] Both studies proposed structures exhibiting end-on (η^1) binding of dioxygen to Cu_B, with an O—O bond length short enough to discount assignment of the complex as a Cu(III)-peroxide or Cu(III)-hydroperoxide intermediate. Recent mixed quantum mechanics/molecular mechanics (QM/MM) calculations on the DβM system (constructed by homology modeling using a PHM crystal structure[11]) also support an end-on coordination mode and primarily superoxo character for the 1:1 Cu_B-O_2 adduct.[14] Further QM/MM calculations[15] as well as calculations on quantum models cropped from the QM/MM structures[14] showed that the Cu(II)-superoxo species was effective at hydroxylating dopamine under physiological conditions. A Cu(III)-oxo species was shown to have even higher oxidative power, suggesting that this unstable intermediate could play a role in catalysis if it indeed forms at the DβM active site.[14,15] The finding that the $^{18}O_2$ kinetic isotope effect in the DβM system is influenced by substrate deuteration, however, argues against the involvement of the Cu(III)-oxo.[9,16] Other calculations on PHM active site models have suggested a Cu(II)-hydroperoxide or a side-on (η^2) bound copper–oxygen complex intermediate in character between Cu(II)-superoxo and Cu(III)-peroxo as alternative intermediates and further inferred that the η^2 Cu-O_2 complex is the reactive species in PHM.[17,18]

The chemistry of the Cu_B sites in DβM and PHM has also been approached using putative biomimetic model systems.[19] Tripodal tetradentate ligands, such as tris(2-pyridylmethyl)amine,[20,21] tris(2-pyridylethyl)amine,[21] tris(tetramethylguanidino)tren,[22] and a bisamide functionalized polyimidazole ligand,[23] have been demonstrated through a combination of theoretical and experimental evidence to be capable of stabilizing end-on 1:1 Cu-O_2 adducts. We focus here instead on two monoanionic bidentate ligands from Tolman et al. (Scheme 1), a β-diketiminate (L^1) and an anilido-imine (L^2), which have the virtue of more closely reproducing the coordination environment of Cu_B in DβM and PHM, in which only two nitrogen donors (histidine residues) are present.[10,11,24–27] These ligand systems have likewise shown the ability to stabilize 1:1 Cu-O_2 adducts.[28,29] Characterized both experimentally and theoretically, these complexes exhibit side-on binding of dioxygen to the copper center and significant Cu(III)-peroxo character. In addition, the mechanism of dioxygen activation within the β-diketiminate system has been elucidated using a combination of experimental and computational methods.[28] Despite these promising developments, the 1:1 Cu-O_2 adducts yielded by these two ligand systems have proven to be unreactive toward a wide range of exogenous organic substrates in neutral or acidic solutions.[30] To design the next generation of ligands for biomimetic models of DβM and PHM, the reactivity of these 1:1 adducts must be explained, and that is the subject of this work.

We begin by determining the dioxygen activation mechanism in the anilido-imine ligand system and comparing it to the β-diketiminate case.[28] We next compute pK_b values and reduction potentials for the 1:1 Cu-O_2 adducts supported by L^1 and L^2 and for derivative Cu(III)-hydroperoxide, Cu(III)-oxo, and Cu(III)-hydroxide species. Trends in these properties explain the relative reactivity of these species with hydrocarbon substrates. Hydrogen-atom abstraction transition-state structures are examined to confirm these conclusions. Implications for the design of new biomimetic models and insights into the catalytic cycles of DβM and PHM are addressed.

Computational Methods

Density Functional Calculations

Geometry optimizations were carried out using the Jaguar suite, version 5.0, of *ab initio* quantum chemistry programs.[31] Density functional theory (DFT) with the B3LYP functional,[32–34] which has been shown to successfully predict ligand-Cu(I) and -Cu(II) bond dissociation energies,[35] was applied for all geometry optimizations. Singlet and triplet states were treated at restricted (RDFT) and unrestricted (UDFT) levels of theory, respectively, in keeping with the established methodology for the types of copper–oxygen complexes described herein.[13,28,29,36,37] In addition, UDFT methods were used for doublets and optimizations of Cu(III)-hydroxide complexes. Basis sets utilized included the lacvp** effective core potential basis for Cu[38–40] and the double-ζ plus polarization (DZP) 6-31G** basis for all other atoms. Reaction coordinate profiles were obtained by freezing at least one interatomic distance and optimizing all other degrees of freedom. The quadratic synchronous transit method was used for all transition-state searches.[41] Mulliken charge and spin populations and natural

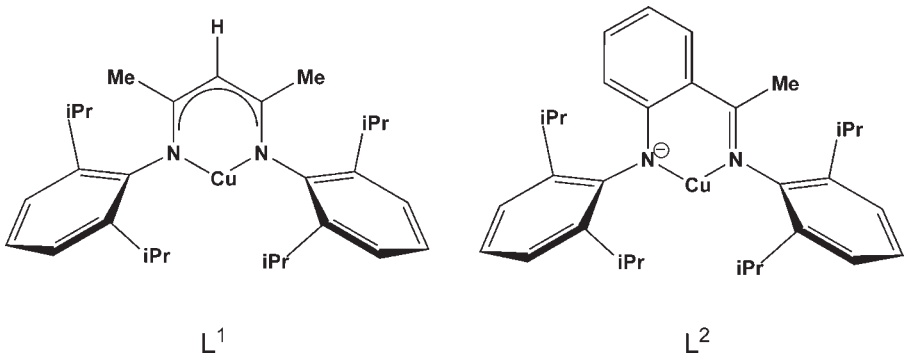

L^1 L^2

Scheme 1.

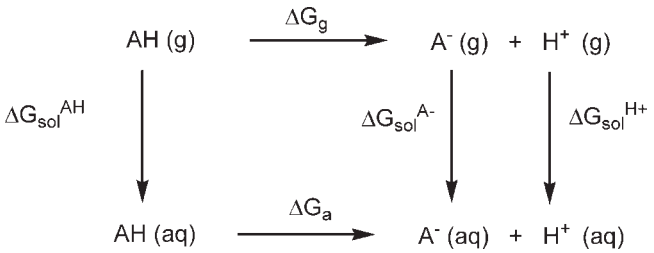

Scheme 2.

population analysis (NPA) partial atomic charges[42] have been computed and used to track electronic changes along reaction coordinates and between closely related structures. Mulliken population analyses have proven to be a convenient method of tracking electron flow in other systems involving the reaction of dioxygen at a metal center and hydrogen-atom abstraction by the subsequently formed metal–oxygen complexes.[43,44]

The B3LYP/DZP optimized geometries and transition state structures were verified as such by analytical vibrational frequency calculations. These calculations enabled zero-point, enthalpy, and entropy corrections to be made to the electronic energies, thus allowing free energies to be determined. The zero-point, enthalpy, and entropy corrections as well as electronic energies, CASPT2 corrections, and solvation energies for all computed species can be found in the Supporting Information (Table S2). To render these calculations computationally tractable, truncated models in which the four isopropyl groups are replaced with hydrogen atoms (whose positions were optimized while keeping the remainder of the structure frozen) were used in the vibrational frequency computations. The error introduced through this approximation is expected to be nominal, as the isopropyl groups do not directly participate in the chemistry taking place at the copper center (*vide infra*). The steric and electronic influences that are exerted by the isopropyl groups are accounted for within the geometry optimizations, which are performed using the entire L^1 and L^2 ligands. Reported vibrational frequencies are scaled by 0.9614.[45]

Single-point solvation energies for optimized geometries were calculated using the self-consistent reaction field method as implemented in the Poisson–Boltzmann solver in Jaguar.[46,47] Values for the dielectric constant ε of THF (used as the solvent to facilitate comparison to experimental data) were taken to be 7.43 at 25°C and 10.42 at −50°C.[48,49] For free-energy changes computed in solution, a translational entropy correction was included to account for the change in concentration from the 1 atm gas-phase (determined as 1/24.5 M from the ideal gas law) to the 1 M standard-state solution concentration.[50] Where solvent THF was an explicit participant in a chemical reaction, solvent concentration, calculated from the pure liquid density,[48,49] was factored into the entropy correction.

pK_b values were determined through the use of a Born–Haber free-energy cycle (Scheme 2). The free-energy change for deprotonation in aqueous solution is

$$\Delta G_a = \Delta G_g - \Delta G_{sol}^{AH} + \Delta G_{sol}^{A-} + \Delta G_{sol}^{H+} \quad (1)$$

where ΔG_g is the gas-phase deprotonation energy and ΔG_{sol}^{AH}, ΔG_{sol}^{A-}, and ΔG_{sol}^{H+} are the solvation free energies for the conjugate acid and base forms and the proton, the latter of which is taken to be −265.9 kcal/mol prior to correcting for the 1-atm to 1-M standard-state change.[51,52] The pK_b is then calculated as

$$pK_b = 14.0 - \frac{\Delta G_a}{2.303RT} \quad (2)$$

where R is the universal gas constant and T is temperature.

Adiabatic reduction potentials have also been calculated using a free-energy cycle (Scheme 3). The free-energy change for reduction in solution ΔG_r is

$$\Delta G_r = G_g^{X-} - G_g^{X} + \Delta G_{sol}^{X-} - \Delta G_{sol}^{X} \quad (3)$$

where G_g^{X-} and G_g^{X} are the gas phase free energies for the reduced and oxidized species, and ΔG_{sol}^{X-} and ΔG_{sol}^{X} are the corresponding solvation energies. The absolute reduction potential is determined as

$$E^o = -\frac{\Delta G_r}{nF} \quad (4)$$

where F is the Faraday constant and n is the number of electrons transferred. The potential relative to the standard hydrogen electrode (SHE) can be obtained by subtracting 4.28 V[52] from the quantity in eq. (4). An empirical correction was employed to compensate for systematic error involved in the computation of the reduction potentials. A copper complex supported by a triazamacrocyclic ligand, with the rare combination of possessing a similar coordination chemistry to that of L^1 and L^2 and having been well characterized in terms of its electrochemistry, and a measured Cu(III)/Cu(II) reduction potential of −0.271 V *versus* SHE was taken as a reference point.[53] Calculations indicate this reduction potential to be 0.485 V, leading to a correction factor of −0.76 V. Transferability of such corrections between closely related systems has been shown to be a viable approach.[54]

Bond dissociation energies (BDEs) were calculated for the homolytic bond cleavage reactions R—H → R·+H·. To determine C—H BDEs for the benzylic position in dopamine and the C_α position in formylglycine (which are not readily available in the literature), C—H BDEs were first calculated for a variety of hydrocarbons with C—H bond strengths ranging from 104.9 kcal/

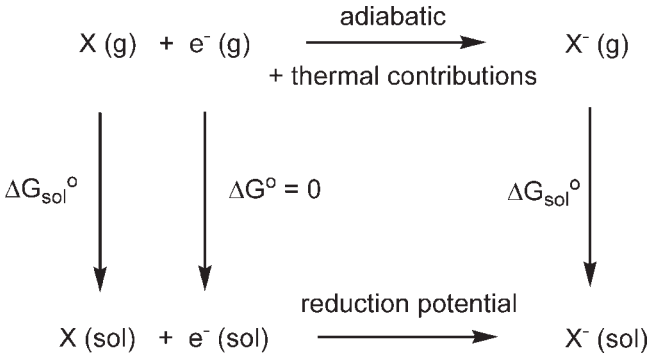

Scheme 3.

mol (methane) to 73.0 kcal/mol (1,4-cyclohexadiene).[55] The calculated values were then linearly correlated against tabulated values[55] so as to yield a relationship between computed and literature BDEs (see Supplementary Fig. S1). This correction (on the order of 2 kcal/mol) was then applied to the BDEs computed for dopamine and formylglycine.

Multireference Calculations

In contrast to closed-shell singlet and high-spin triplet Kohn-Sham wave functions (which can be expressed as single Slater determinants), open-shell singlets require at least two determinants and thus cannot be rigorously represented within the framework of Kohn-Sham DFT. This limitation is particularly relevant for computations on Cu-O_2 adducts (in particular, L^1CuO_2,[36] $L^1CuO_2H^+$, and the L^2 analogs) and Cu(III)-oxo species. The latter may possess significant Cu(II)-oxyl character, while significant Cu(II)-superoxo character in the former has been documented to lead to sizable errors in singlet energies computed via DFT methods in a simplified version of the L^1 system.[36] In each case, the result is electronic states that resemble a biradical with one electron localized to copper and another localized to the oxygen moiety. Single-point multireference second-order perturbation theory (CASPT2) calculations[56] have been carried out to account for the multideterminantal nature of the singlet Cu-O_2 adducts and Cu(III)-oxo species when calculating energies and singlet-triplet energy differences for these complexes. Broken symmetry unrestricted density functional theory (BS-UDFT) provides another potential method for accounting for, at least in an approximate way, the multideterminantal nature of the species in question. However, the BS-UDFT method proves to be inadequate in the current case. In particular, the BS-UDFT energies (after accounting for spin contamination via spin projection) for the singlet side-on 1:1 Cu-O_2 adducts supported by L^1 and L^2 are higher in energy than the corresponding triplets by 8.3 and 7.5 kcal/mol respectively. By comparison, the singlet RDFT energies are higher in energy than the corresponding triplets by 9.3 and 9.1 kcal/mol respectively. In short, the RDFT and BS-UDFT energies for the singlets are nearly equal and both incorrectly predict a triplet ground state for the side-on 1:1 Cu-O_2 adducts, which are experimentally known to be ground state singlets based upon EPR spectroscopy (cf. Refs. 28 and 29). The MOLCAS program was used for CAS and CASPT2 calculations.[57]

For the Cu-O_2 adducts, the initial complete active space (CAS) of the reference wave function consisted of 18 electrons in 12 orbitals, specifically, the Cu valence electrons/orbitals and the O_2 σ_{2p}, σ^*_{2p}, π_{2p}, and π^*_{2p} electrons/orbitals. A final (12,9) active space was achieved by removing orbitals with occupation numbers greater than 1.999.[36] The initial CAS for the Cu(III)-oxo species comprised 16 electrons in 10 orbitals stemming from the Cu(III) valence electrons (8) and orbitals and the 8 electrons and 4 orbitals of O^{2-} with principal quantum number 2. After eliminating doubly occupied orbitals, a final (10,7) active space was arrived at for these calculations.

For the β-diketiminate ligand case,[28] a 17-electron relativistic effective core potential basis was used for Cu,[58] and a polarized double-ζ atomic natural orbital basis was used for all other atoms.[59] In calculations on the anilido-imine ligand system, internal charge separation is larger because of the formal localization of the ligand anionic charge onto one Cu-coordinating nitrogen atom.[29] Consequently, for these cases, a 17-electron relativistic effective core potential with a polarized valence triple-ζ (TZP) basis set for the valence electrons was used for Cu,[58] and a TZP atomic natural orbital basis set was used for O, N, and H (N—H) atoms,[59] while in the interest of keeping the CASPT2 calculations tractable, C was treated with the 3-21G basis[60] and remaining H atoms with the STO-3G basis.[61]

The significant inherent computational expense of the CASPT2 methodology renders such calculations on the full L^1 and L^2 systems impractical and mandates instead the use of simplified versions of the L^1 and L^2 ligand systems for these calculations. This is achieved by changing the backbone methyl group(s) and the 2,6-diisopropylphenyl flanking groups to hydrogen atoms. The difference Δ in the singlet–triplet energy splittings calculated at the DFT and CASPT2 levels for these simplified models is

$$\Delta = ({}^1A - {}^3A)_{\mathrm{CASPT2}} - ({}^1A - {}^3A)_{\mathrm{DFT}} = [({}^1A)_{\mathrm{CASPT2}} - ({}^1A)_{DFT}] - [({}^3A)_{\mathrm{CASPT2}} - ({}^3A)_{\mathrm{DFT}}]. \quad (5)$$

As triplet states are well described by single-determinantal methods like DFT, the relative energy difference for the triplet between the two levels of theory may be taken to be zero. Equation (5) then yields the relative difference in the singlet energies between DFT and CASPT2, and the quantity Δ can be interpreted as a CASPT2-based correction to the singlet energy provided by DFT. Final electronic energies for singlet states for the full ligand systems are obtained by summing the SCF energies from DFT calculations on the full L^1 and L^2 ligand systems with Δ for the corresponding simplified model. This methodology has proved capable of predicting both the proper singlet–triplet state orderings[28,29,37] and the kinetics of oxygenation in the L^1 system.[28] To facilitate the determination of Δ along the reaction path for 1:1

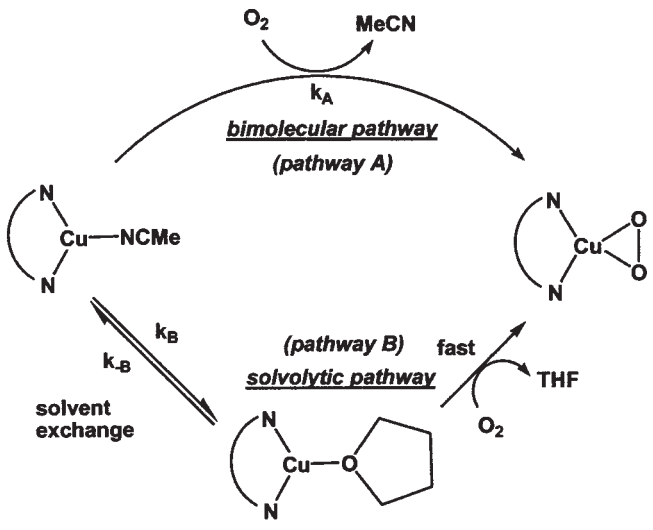

Scheme 4.

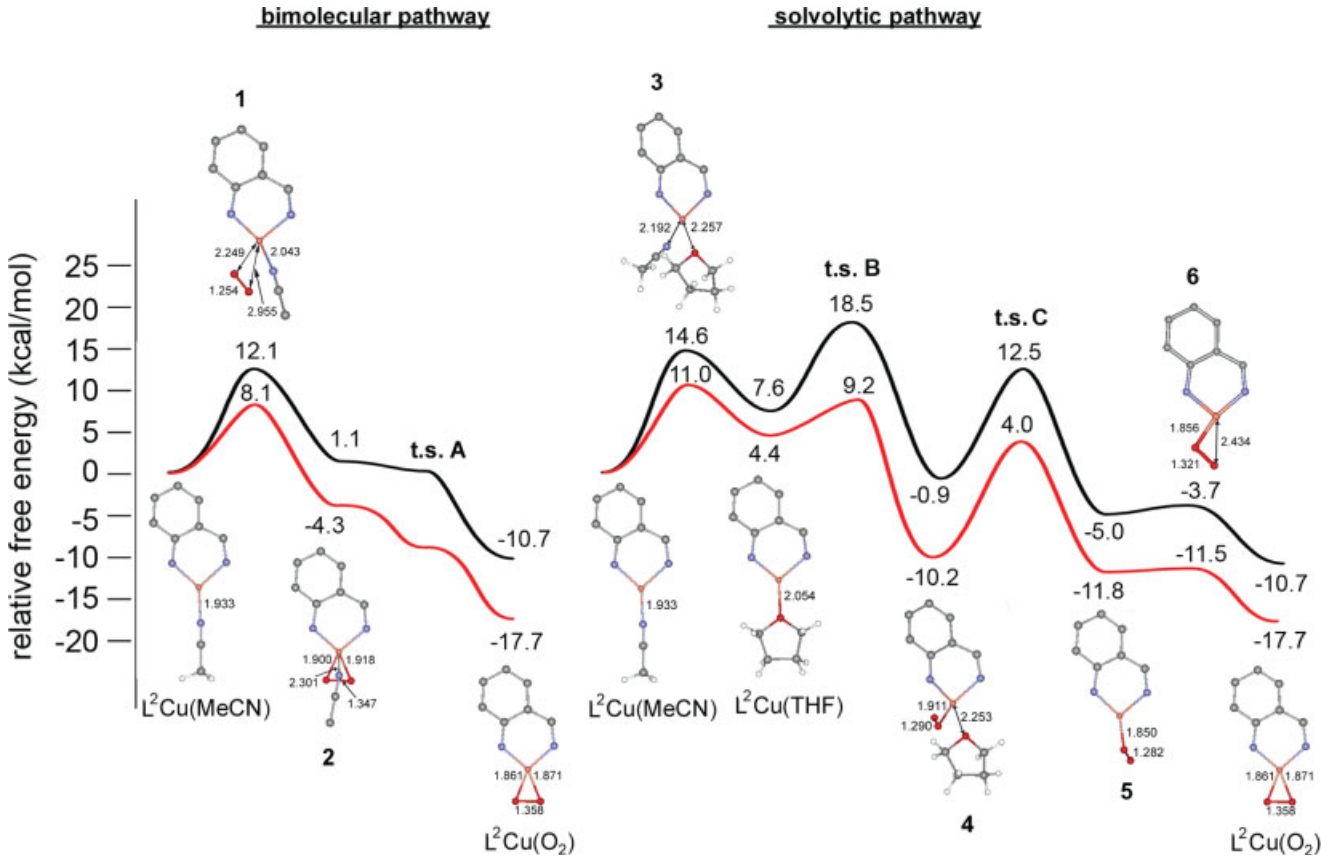

Figure 1. Calculated reaction coordinates for the bimolecular and solvolytic oxygenation mechanisms for the Cu complex supported by L^2 at 25°C/gas phase (black line) and at 223 K/THF (red line). Substituents on L^2 are omitted for clarity. Distances are measured in Å. Pink stands for Cu; gray, C; blue, N; yellow, S; red, O; white, H.

Cu-O_2 adduct formation in the L^2 system, linear correlations between Δ and the Cu—O bond length were determined over a range of 1.86–2.33 Å in the side-on isomer and 1.85–2.15 Å in the end-on isomer (Fig. S2).[28] CASPT2 corrections are then readily determined for any singlet side-on or end-on adduct between these two endpoints. Since the CASPT2 correction at an infinite Cu—O distance should refer only to molecular dioxygen, an extrapolation was employed at longer Cu—O distances to obtain the correct asymptotic limit. Calculations show the correction Δ_{O_2} (determined analogously as in eq. (5)) for singlet dioxygen (specifically, the lowest energy singlet state $^1\Delta_g$) to be 15.0 kcal/mol. The long-range extrapolated CASPT2 correction is then

$$(\text{max correction} + \Delta_{O_2})\left(\frac{O-O-1.215}{O-O_{max}-1.215}\right) - \Delta_{O_2} \qquad (6)$$

where "max correction" refers to the CASPT2 correction at the last point in the linear correlations, $O–O_{max}$ and O–O are the oxygen–

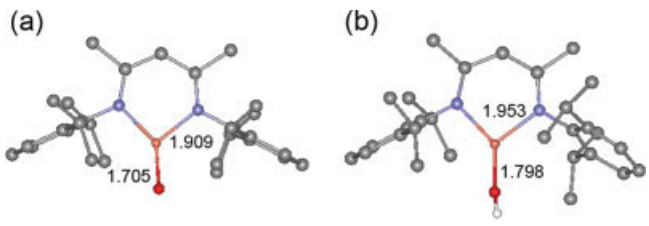

Figure 2. Optimized geometries for (a) L^1CuO and (b) L^1CuOH^+. Hydrogen atoms on L^1 are omitted for clarity. Distances are measured in Å. Pink stands for Cu; gray, C; blue, N; yellow, S; red, O; white, H.

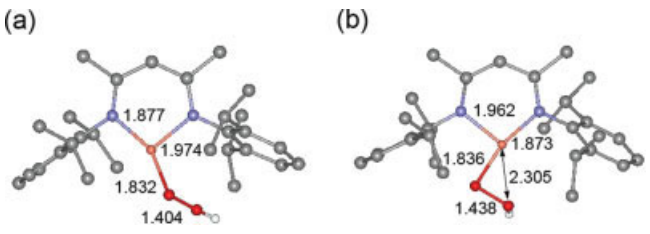

Figure 3. Optimized geometries for (a) end-on $L^1CuO_2H^+$ and (b) side-on $L^1CuO_2H^+$. Hydrogen atoms on L^1 are omitted for clarity. Distances are measured in Å. Pink stands for Cu; gray, C; blue, N; yellow, S; red, O; white, H.

Table 1. Activation Parameters at 223 K in THF for the Oxygenation Reactions of the Cu(I)/MeCN Complexes Supported by L^1 and L^2.

	$\Delta G^{\ddagger}$ (kcal/mol)	$\Delta H^{\ddagger}$ (kcal/mol)	$\Delta S^{\ddagger}$ (cal/(mol K))
Pathway A			
L^1 Theory[28]	9.3	3.6	−25.8
L^1 Experiment[28]	8.9–9.7	4.3	−23.9
L^2 Theory	8.1	1.7	−28.6
Pathway B			
L^1 Theory[28]	11.9	6.5	−24.1
L^1 Experiment[28]	12.3–12.4	7.2	−23.7
L^2 Theory	11.0	4.1	−31.2

oxygen bond lengths at the last point in the correlations and in the particular elongated Cu—O structure, respectively, and 1.215 Å is the calculated equilibrium triplet dioxygen bond length.

Results

Dioxygen Activation Mechanism in the L^2 System

Kinetics experiments examining oxygenation of L^1Cu(MeCN) revealed that two reaction pathways (Scheme 4) are possible, depending on whether the reaction is carried out in neat THF or in THF/MeCN mixtures.[28] Structures and free energies for intermediates and transition states along both the bimolecular and solvolytic pathways in the L^2 system are shown in Figure 1. Activation parameters for both pathways in the L^2 case are very close to those determined experimentally and theoretically when L^1 is the supporting ligand (Table 1).[28] The overall oxygenation reaction is also exergonic, as in the L^1 case. Reduction of dioxygen in the 1:1 adducts supported by both L^1 and L^2 results from the flow of electron density in nearly equal amounts from the Cu center and the anionic β-diketiminate and anilido-imine ligands based upon analysis of the Mulliken and NPA charges.

Not surprisingly therefore, the essential features of the bimolecular oxygenation mechanism from the L^1 system[28] are mirrored in the L^2 system: (1) a dissociative mechanism is computed to have a higher activation barrier, in the case of L^2 by 11.8 kcal/mol at 25°C in the gas phase; (2) the associative mechanism features a rate-determining transition state on the triplet surface exhibiting weak end-on coordination of dioxygen to the copper center; and (3) while an L^2Cu(MeCN)(O_2) structure can be identified, it is not a stationary point under the experimental reaction conditions (223 K, THF). Primary aspects of the solvolytic pathway for oxygenation in the L^1 system are also conserved with L^2: (1) solvent exchange at the Cu site occurs via an associative mechanism, with the alternative dissociative mechanism having a noticeably higher barrier (by 10.5 kcal/mol at 25°C in the gas phase for L^2); (2) the solvent interchange segment of the reaction is endergonic, consistent with MeCN as a strongly coordinating ligand and THF as a weakly coordinating ligand to Cu(I); (3) the reaction of L^2Cu(THF) with dioxygen proceeds through an associative mechanism and involves the formation of an unstable singlet L^2Cu(THF)(O_2) intermediate with η^1 dioxygen coordination; and (4) the rate-determining step changes from dioxygen binding to solvent exchange in going from 25°C and gas phase to the experimental conditions of 223 K and THF solvent.

Cu(III)-oxo Species

Addition of 2 protons and 2 electrons to the 1:1 Cu-O_2 adducts may in principle lead to O—O bond cleavage, release of a water molecule, and production of an intermediate that may be formally termed a Cu(III)-oxo species. Computed potentials for this reduction half-reaction

$$LCuO_2 + 2H^+ + 2e^- \rightarrow LCuO + H_2O \quad (7)$$

at 25°C in H_2O (pH 7) are −1.02 V with L^1 and −0.98 V with L^2 and indicate that this half-reaction would need to be coupled with only a moderately strong reductant (or a strongly acidic environment) to be energetically favorable. These data point toward the accessibility of a Cu(III)-oxo intermediate. They do not, however, suggest a synthetic route to this species, given the likely instability of the Cu(III)-oxo unit in an aqueous medium.[62]

Optimized geometries for the singlet L^1CuO (Fig. 2a) and L^2CuO (Fig. S3a) show a short Cu—O bond length of 1.705 Å, consistent with some degree of multiple bond character, as compared to the Cu—O bonds in the 1:1 adducts, which have lengths of ∼1.85 Å. On the other hand, the Cu—O bond lengths in LCuO compounds are longer than those typically observed for monooxo compounds of other first row transition metals (∼1.57−1.64 Å).[63] The Cu-oxo stretch frequencies in LCuO (704 cm^{-1} with L^1, 697 cm^{-1} with L^2) are also lower than the typical 900–1000 cm^{-1} for ν(M—O).[64] The relatively weak copper-oxo bond in LCuO can be attributed to the population of a metal-oxo π^* orbital.[62] Occupation numbers of 1.45 and 0.55 for the two partially occupied orbitals (Fig. S4) in the CASPT2 calculations for L^1CuO support this overall view of the electronic structure and more specifically identify the species to be virtually intermediate between Cu(II)-O· character (occupation numbers of 1.00 and 1.00) and Cu(III) = O character (occupation numbers of 2.00 and 0.00). The geometry for L^2CuO also shows that the asymmetry associated with the L^2 ligand system does not translate into asymmetric binding of the oxo moiety to the copper center.[29] The triplet LCuO structures have higher free energies at 25°C in the gas phase than the singlets for both L^1 (ΔG = 5.8 kcal/mol) and L^2 (ΔG = 13.5 kcal/mol).

Neither L^1CuO nor L^2CuO has been isolated, possibly because of the weaker metal–oxygen bonding than is seen in stable compounds of group 5–8 transition metals with terminal oxo ligands

Table 2. Free Energies (kcal/mol) for $LCuO_2H^+$ Species Relative to the End-On Singlet State at 223 K in THF.

	L^1	L^2
Side-on singlet	+15.4	+3.1
Side-on triplet	+10.2	+8.7
End-on singlet	0.0	0.0
End-on triplet	+7.9	+7.6

Table 3. Reduction Potentials (25°C, THF) and pK_b (25°C, H_2O) Values for Copper–Oxygen Complexes and Gas Phase O—H Bond Dissociation Energies for Copper–Oxygen Complexes for a Hydrogen Atom Bound to the Oxygen Moiety.

	E^O (V)	pK_b	BDE (kcal/mol)
η^2-L^1CuO_2	−2.06	14.1	54.9
η^1-L^1CuO_2	−1.92	10.5	60.9
$L^1CuO_2H^+$	−0.20	36.7	43.2
L^1CuO	−1.65	−4.7	99.7
L^1CuOH^+	0.28	4.9	99.0
η^2-L^2CuO_2	−2.26	16.2	46.6
η^1-L^2CuO_2	−2.05	12.4	56.9
$L^2CuO_2H^+$	−0.43	34.6	38.7
L^2CuO	−2.04	−1.3	92.1
L^2CuOH^+	0.08	5.3	87.5

and/or these species' anticipated high reactivities.[62] A Cu(III)-oxo species has been postulated as an intermediate resulting from cleavage of the O—O bond of a μ-peroxo binuclear complex $(LCu)_2O_2$, L = $HB(3,5\text{-}Me_2pz)_3$, but to our knowledge, no direct spectroscopic evidence for such a species has been obtained.[65,66]

Characterization of the Copper/Oxygen Complexes

Cu(III)-hydroperoxide and Cu(III)-hydroxide

Relative free energies of the side-on and end-on singlet and triplet protonated 1:1 Cu-O_2 adducts are shown in Table 2. For both the L^1 and L^2 cases, the end-on singlet is energetically preferred and features an O—O distance of 1.404 Å in the L^1 system (Fig. 3a) and 1.417 in the L^2 system (Fig. S5a). These bond lengths are 0.05 Å longer than in the η^2 $LCuO_2$ structures and 0.13 Å longer than in the η^1 $LCuO_2$ structures. This is consistent with the increase in the Mulliken charge population on the O_2 unit by ~0.1 eu (with the NPA charges, by ~0.2 eu) upon protonation and with this new electron density inhabiting the heretofore partially occupied oxygen π^* orbitals. Both the bond lengths and associated ν(O—O), 936 cm^{-1} for L^1 and 911 cm^{-1} for L^2, support the assignment of $LCuO_2H^+$ as Cu(III)-hydroperoxide, albeit narrowly in peroxide territory beyond the superoxide–peroxide continuum.[67]

CASSCF calculations on η^1 $L^1CuO_2H^+$ show the multiconfigurational nature of the wave function for this species. Two orbitals have significant partial occupations (Fig. S6) and are consistent with the formal assignment of the species as Cu(III)-hydroperoxide. Notably, the side-on singlet supported by the β-diketiminate ligand is ~10 kcal/mol less stable than its anilido-imine counterpart. Comparison of the partially occupied orbitals in these cases (Fig. S7) reveals η^2 $L^2CuO_2H^+$ to be Cu(III)-hydroperoxide-like, similar to the η^1 $LCuO_2H^+$ case, while η^2 $L^1CuO_2H^+$ retains a small degree of superoxide character.

The species obtained by protonating Cu(III)-oxo $LCuOH^+$ was computed using only unrestricted DFT methods (see Computational Methods). This proved to be a unique case where singlet UDFT wave functions with limited spin contamination could be obtained, in contrast to the situation with the 1:1 Cu-O_2 adducts.[36] The O—H bond distances in the optimized geometries for $LCuOH^+$, 1.798 Å with L^1 and 1.796 Å with L^2, were in agreement with copper-hydroxide distances determined by experimental[68] and high-level *ab initio* methods.[69] As with $LCuO_2H^+$, the magnitude of Mulliken and NPA charge populations for the oxygen atom in the Cu(III)-hydroxide is increased by ~0.1 eu and ~0.2 eu, respectively, *versus* its conjugate base.

Reduction Potentials and pK_b Values

Reduction potentials (at 25°C, in THF, *versus* the standard hydrogen electrode) and pK_b values (at 25°C, in H_2O) have been computed for all copper–oxygen species discussed earlier, i.e., side-on and end-on 1:1 adducts, Cu(III)-hydroperoxides, Cu(III)-oxos, and Cu(III)-hydroperoxides supported by L^1 and L^2 (Table 3). Trends are consistent between the two ligand systems, with the L^1 complexes 0.25 V easier to reduce and ~1.5 pK_b units easier to protonate than their L^2 analogs.

Comparing neutral species, LCuO is more readily reduced than either isomer of $LCuO_2$. This contrast in reduction potentials tracks the differing degrees of radical character in their oxygen moieties. LCuO has significant Cu(II)-oxyl character, η^1-$LCuO_2$ is intermediate between Cu(III)-peroxo and Cu(II)-superoxo, and η^2-$LCuO_2$ is largely Cu(III)-peroxo in character. Among the positively charged species (which are, of course, inherently easier to reduce than the neutral species), $LCuOH^+$ has a higher reduction potential than $LCuO_2H^+$. The data set as a whole indicates that the monooxygen complexes are more readily reduced than the dioxygen complexes by ~0.5 V.

The most basic neutral species among those examined is LCuO. The other neutral complexes, the 1:1 adducts, have considerably higher pK_b values. Although the oxygen atom in LCuO and the dioxygen moiety in the 1:1 adducts have virtually equal Mulliken and NPA charge populations, it is the concentration of that charge on the one oxygen in LCuO which serves to enhance its basicity.[62] The high pK_b of $LCuO_2H^+$ *versus* $LCuOH^+$ mirrors the trend seen in the relative pK_b values of $LCuO_2$ and LCuO. Although doubly

Table 4. Free Energies of Activation and Reaction (kcal/mol) at 223 K in THF for Isomerization from η^1 to η^2 Coordination of the Dioxygen Moiety.

	$\Delta G^{\ddagger}$	ΔG
L^1CuO_2 (singlet)	+3.4	−4.7
$L^1CuO_2H^+$[a]	~+14	+10.3
$L^1CuO_2^-$ (doublet)	+3.5	−2.1
L^1CuO_2H (doublet)	+2.3	−1.3
L^2CuO_2 (singlet)	+0.3	−5.8
$L^2CuO_2H^+$ (singlet)	+10.3	+3.1
$L^2CuO_2^-$ (doublet)	+6.1	+2.9
L^2CuO_2H (doublet)	+4.4	−0.2

Spin states are indicated in parentheses.

[a]Spin-crossing occurs in going from the most stable η^1 geometry (singlet) to the most stable η^2 geometry (triplet).

Table 5. C—H Bond Dissociation Energies (kcal/mol) for Substrates.

Substrate	BDE
Methane	104.9[a]
Cyclohexane	95.5[a]
Acetonitrile	93.9[a]
Toluene	89.8[a]
Phenol	86.5[a]
Isopropylbenzene	84.4[a]
1,4-Cyclohexadiene	73.0[a]
Formylglycine	86.5[b]
Dopamine	87.2[b]

[a]Ref. 55.
[b]See Computational Methods for calculation procedure.

protonating one of the oxygen atoms in $LCuO_2$ may be considered a prelude to O—O bond cleavage, which is favorable (*vide supra*), it can be concluded that the mechanism for bond cleavage would not begin with successive protonation steps, in particular based upon the pK_b value of $\sim$35 for the $LCuO_2H^+$ intermediate.

η^1/η^2 *Isomerizations*

Relative free energies of the end-on and side-on isomers of the copper-dioxygen complexes—1:1 adducts, Cu(III)-hydroperoxides, and these species' 1-electron reduced forms—show the two isomers to be close in energy in nearly all cases (Table 4). The only exception is $L^1CuO_2H^+$, where the η^2 isomer is singularly high in energy as noted earlier. The barriers for interconversion are also small except in the Cu(III)-hydroperoxide cases. Any changes between η^1 and η^2 dioxygen coordination, as might occur during the substrate hydroxylation process, should thus generally have a minor effect on the activation energy or free-energy change for the reaction.

Reaction with Substrates

Predicting Reactivity

The initial step in the hydroxylation of substrates by DβM, PHM, or biomimetic systems involves hydrogen-atom abstraction from the C—H bond of a substrate by the oxygen moiety of a copper–oxygen complex. The facility with which this reaction step occurs can be analyzed from two different but related viewpoints. First, hydrogen-atom abstraction can be decomposed into its components: transfer of a proton and transfer of an electron from substrate to oxygen.[70] The more favorable each of these component reactions is, the more favorable H-atom abstraction will be. Higher reduction potentials and lower pK_b values (Table 3) for LCuO and $LCuOH^+$ compared to $LCuO_2$ and $LCuO_2H^+$, respectively, indicate higher reactivity for the two monooxygen intermediates.

Second, the relative strengths of the copper–oxygen complexes for H-atom abstraction can be quantified by examining the O—H bond dissociation energies (BDEs) for the new O—H bonds formed following H-atom abstraction (Table 3). The two ligand systems show similar variations in O—H BDEs among the different copper–oxygen species. The BDEs in the L^2 system are, however, consistently $\sim$5 kcal/mol weaker than with L^1, indicating that the β-diketiminate ligand yields copper–oxygen complexes that are slightly more reactive with respect to substrate hydroxylation.

In contrast to this small difference resulting from ligand modification, a much larger variation in O—H BDEs is seen when the nature of the copper–oxygen species is modified. The O—H BDEs for LCuO and $LCuOH^+$ are 30–45 kcal/mol larger than with the 1:1 adducts and Cu(III)-hydroperoxide species. Confirming that addition of acid to the 1:1 adducts to promote reaction with substrates is ineffective,[30] the O—H BDEs are in fact lowest for the Cu(III)-hydroperoxides. The low BDEs for the 1:1 adducts are also consistent with their observed lack of reactivity.[30] LCuO and $LCuOH^+$ should thus react more readily with substrates based on their high O—H BDEs, which stem from their greater reduction potentials and basicities compared with the dioxygen containing species.

Table 6. Enthalpies of Activation, Computed with the Bound Substrate-L^1CuX Complexes as the Reactant, in the Gas Phase, 25°C (kcal/mol) for the Hydrogen Abstraction Reaction Between Substrates and Oxygenated L^1Cu Species.

Substrate	η^2-L^1CuO_2	η^1-L^1CuO_2	$L^1CuO_2H^+$	L^1CuO	L^1CuOH^+	Average per substrate
Methane	46.4	45.3	59.2	14.7	23.0	37.7
Cyclohexane	39.2	35.7	41.3	10.2	10.4	27.4
Acetonitrile	45.2	48.2	57.5[a]	16.6	33.0	40.1
Toluene	37.6	39.8	38.5	11.9	5.1	26.6
Phenol	28.5	43.2	16.7	26.9	NA[b]	28.8
Isopropylbenzene	39.3	38.9	39.4	11.7	14.4	28.8
1,4-Cyclohexadiene	26.8	29.8	28.2	5.8	−1.7[c]	17.8
Formylglycine	22.0[a]	30.6	30.7	14.0	6.8	20.8
Dopamine	36.5	36.5	42.7	24.8	0.2	28.2
Average per copper–oxygen species	35.7	38.7	39.4	15.2	11.4	

[a]Enthalpy of transition state versus that of the infinitely separated reactants. Infinitely separated reactants were lower in energy than the substrate-L^1CuX complexes in these cases.
[b]A transition state for this case could not be obtained.
[c]The negative enthalpy of activation here arises from the zero-point energy correction in this case being larger in magnitude than the (positive) electronic energy of activation.

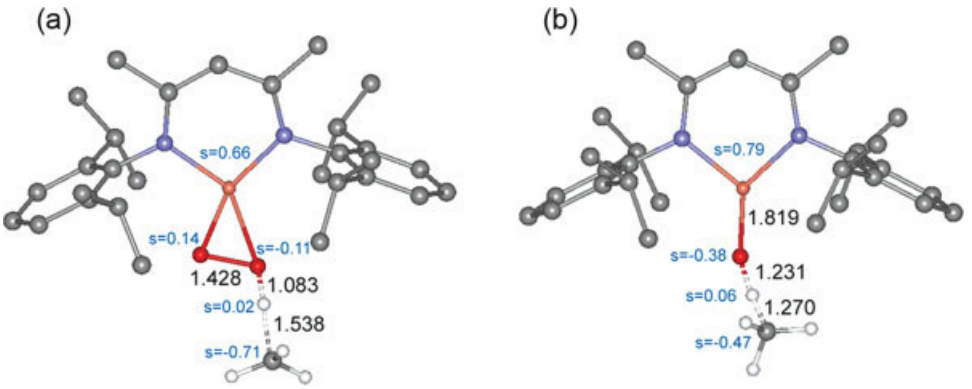

Figure 4. H-atom abstraction transition states for the reaction of methane with (a) η^2-L^1CuO_2 and (b) L^1CuO. Hydrogen atoms on L^1 are omitted for clarity. Mulliken spin populations are denoted by "*s*=." Top-most spin population refers to the LCu fragment; bottom-most, to the nascent substrate radical. Distances are measured in Å. Pink stands for Cu; gray, C; blue, N; yellow, S; red, O; white, H. [Color figure can be viewed in the online issue, which is available at www.interscience.wiley.com.]

Comparison of the O—H BDEs with substrate C—H BDEs (Table 5) allows the free energies of reaction between each copper–oxygen complex and a range of substrates to be quantified. For the 1:1 adducts and Cu(III)-hydroperoxides, the O—H BDEs are lower than the C—H BDEs of all potential substrates by at least 30 kcal/mol, again confirming the nonreactivity of these species. LCuO and $LCuOH^+$, on the other hand, are sufficiently potent to react with a wide range of potential substrates, including dopamine and formylglycine (a PHM substrate analog).[18]

Hydrogen-Atom Abstraction Transition States

To confirm the predicted trends in energetics of hydrogen atom abstraction among different copper–oxygen species and different substrates, hydrogen atom transition-state structures and activation enthalpies (calculated with bound substrate/copper–oxygen complexes as the reactant) were computed (Table 6). Only copper–oxygen complexes supported by L^1 were examined here, since L^2 analogs were extremely similar in terms of reduction potentials, pK_b values, and O—H BDEs.

Activation enthalpies are markedly lower (by ~20–25 kcal/mol on average) for the L^1CuO and L^1CuOH^+ cases compared with that for L^1CuO_2 and $L^1CuO_2H^+$, confirming the predicted higher reactivity of the former. In keeping with the minimal O—H BDE for $L^1CuO_2H^+$, the average activation enthalpies are highest for this case.

Reactions involving substrates with the strongest C—H bonds, such as methane and acetonitrile, lead to the largest $\Delta H^‡$ values. The lowest average $\Delta H^‡$ occurs for the case with the weakest C—H bond, 1,4-cyclohexadiene. Toluene, phenol, and isopropylbenzene have approximately equal and intermediate C—H bond strengths, and this is reflected in their moderate and nearly equal average $\Delta H^‡$. Dopamine likewise falls within the midrange for C—H BDEs and activation enthalpies. Formylglycine reactions proceed with lower barriers as the anionic charge borne by formylglycine is stabilized, as that charge is partially delocalized onto the copper–oxygen species at the transition state.

Examination of the hydrogen-atom abstraction transition states for substrates (e.g., methane) reacting with copper–oxygen complexes at each end of the O—H BDE spectrum (e.g., η^2-L^1CuO_2 and L^1CuO) reveal how the activation-enthalpy differences manifest themselves geometrically and electronically. Both transition states (see Fig. 4) are nearly linear ($\angle C—H—O = 166.9°$ with η^2-L^1CuO_2 and $\angle C—H—O = 173.5°$ with L^1CuO), as would be expected for hydrogen-atom abstraction, and appear to be good models for the analogous reaction in PHM, which exhibits a large primary deuterium kinetic isotope effect.[71] In accordance with the Hammond postulate for a reaction with a large activation enthalpy, the transition state for the poor oxidant η^2-L^1CuO_2 is late, with a C—H distance of 1.538 Å (cf. 1.093 Å in methane) and an O—H distance of 1.083 Å (cf. 0.970 Å in η^2-L^1CuO_2H). The transition state with the much more powerful oxidant L^1CuO occurs early to midway along the reaction coordinate between reactant and hydrogen-abstracted product for the reaction with methane. By tracking Mulliken spin populations, the degree of electron transfer from substrate at the transition state can be seen to parallel with the geometric differences between the η^2-L^1CuO_2 and L^1CuO cases. In particular, in the former, ½ – ⅔ of an electron is transferred from methane to η^2-L^1CuO_2 at the transition state, with ~25% of the electron density accumulating on the L^1Cu unit and the remainder on the dioxygen moiety. Alternatively, at the L^1CuO transition state, only ⅓ – ½ of an electron is transferred from methane, and of that electron density, ~75% resides on L^1Cu and ~25% on the O atom. This is consistent with the L^1CuO reaction being driven primarily by the far greater basicity of the Cu(III)-oxo compared to that of the 1:1 adduct.

Implications for Biomimetic Modeling and DβM and PHM Catalysis

Biomimetic Modeling

Low O—H BDEs and high activation energies for H-atom abstraction by the η^2 1:1 adducts corroborate the experimentally ob-

served lack of reactivity of these complexes with substrates.[30] As noted earlier, the inertness of the 1:1 adducts stems from their low reduction potentials and low basicities (as measured by pK_b values). In order for the next generation of DβM and PHM biomimetic model systems not only to bind dioxygen but also to exhibit reactivity toward substrates, they would have to be more susceptible to both protonation and 1-electron reduction.

The reduction potential of the 1:1 adduct could be increased by shifting the character of the side-on bound 1:1 adduct from primarily Cu(III)-peroxo to primarily Cu(II)-superoxo. This in turn may be achieved by employing a less electron-rich ligand than either the β-diketiminate or anilido-imine ligands. Such a ligand could be created by incorporating electron withdrawing groups on the ligand backbone or flanking steric bulk. Alternatively, a neutral, rather than anionic, ligand could be utilized. One drawback of this approach, however, will be reduced affinity for dioxygen as the LCu unit becomes less electron-rich. Optimal ligand design will involve striking a balance between the need to reduce the electron-rich character of LCu so as to yield a reactive 1:1 adduct while maintaining a sufficiently electron-rich copper center in LCu to make dioxygen binding energetically favorable.

The end-on 1:1 adducts, which have more Cu(II)-superoxo character than the side-on isomers, were shown to have slightly higher reduction potentials and basicities than the side-on 1:1 adducts (cf. Table 3). Combining the above ligand-design principles with a ligand that would also favor η^1 over η^2 dioxygen coordination could lead to further enhancement of reactivity toward substrates.

In conclusion, an ideal biomimetic system would possess only a moderate degree of electron donating character such that dioxygen would bind stably, but still yield a reactive 1:1 adduct and such that end-on binding of dioxygen would be favored over side-on binding. These ligand design strategies are in fact the same as those adopted by nature in DβM and PHM, where the residues which coordinate to Cu_B are all neutral (two histidines and one methionine)[10,11,24–27] and support superoxide-like η^1 dioxygen coordination.[12]

DβM and PHM Catalysis

The results obtained here on the L^1 and L^2 biomimetic model systems provide insights as to which intermediate might be responsible for substrate hydroxylation in DβM and PHM. As suggested in relation to ligand design, a superoxide-like 1:1 adduct should exhibit greater reactivity than intermediates resembling Cu(III)-peroxide. This observation is in accord with the most recent DβM mechanistic proposal positing a Cu(II)-superoxide species as the hydroxylating agent.[9] An end-on Cu(II)-superoxo has also been shown to be effective in this respect in DFT calculations on DβM active side models.[14] Our results do not support an alternative proposal that an η^2 1:1 Cu-O_2 species with a long O—O bond length of 1.387 Å,[18] which in other 1:1 Cu-O_2 adducts has been shown to correspond to species best characterized as intermediate in character between Cu(II)-superoxo and Cu(III)-peroxo and closer to the latter,[28,29,37] could be responsible for hydroxylating substrate in the PHM system.

A potential role for a Cu(III)-oxo/Cu(II)-oxyl intermediate in the DβM and PHM systems may also be suggested based on the present data. If such an intermediate is formed in an enzyme active site, it should be especially capable of carrying out hydrogen-atom abstraction reactions. QM/MM calculations on and active site modeling of the DβM system by Yoshizawa and coworkers have led to similar conclusions.[14,15] Their results indicate that a Cu(III)-oxo is more efficacious for abstracting the benzylic hydrogen from dopamine by $\sim$15 kcal/mol compared with the Cu(II)-superoxo species. A similar trend has been observed here within the L^1 system (cf. Table 6), with differences in absolute values for the activation energies in the two systems likely being attributable chiefly to the difference in the charge of ligands coordinating to copper (i.e., monoanionic with L^1, neutral in DβM). A Cu(II)-oxyl has previously been proposed to be the hydroxylating agent in DβM,[8,72] but more recently reported kinetic evidence argues against this notion.[9,16] As an illustration that a Cu(III)-oxo intermediate might be competent in this regard, a Cu(III)-oxo intermediate with Cu supported by $HB(3,5\text{-}Me_2pz)_3^-$ has been suggested to be capable of hydroxylating cyclohexane, although this hypothesis still awaits direct experimental verification.[65,66]

Unfortunately, the activity of a Cu(III)-oxo species may be difficult to study biomimetically. The same properties that make this species reactive toward substrates also make it a relatively unstable species and difficult to isolate. It is worth noting that this problem has been solved by DβM and PHM, where dioxygen activation occurs only when substrate is bound near the active site.[8,10,73] Should a reactive Cu(III)-oxo be formed, it could react with the prepositioned substrate before having opportunity to engage in a side-reaction.

Conclusions

1:1 Cu-O_2 adducts supported by a β-diketiminate ligand (L^1) and an anilido-imine ligand (L^2) were computationally characterized in an effort to understand their inertness with respect to C—H bond activation reactions, in contrast to the copper-containing enzymes DβM and PHM. Based on these calculations, design features for new ligand systems with improved reactivity were developed. Comparison of the dioxygen-activation mechanisms between L^1 and L^2 revealed them to be essentially the same, with all main mechanistic features being conserved in the two ligand systems and only negligible differences in their energetics.

Alternative copper–oxygen complexes for which the 1:1 adducts may be considered parents were examined, including a Cu(III)-oxo species resulting from O—O cleavage, and Cu(III)-hydroperoxide and Cu(III)-hydroxide species resulting from protonation of the 1:1 adducts and Cu(III)-oxo, respectively. The Cu(III)-oxo was determined to be best characterized as intermediate in character between Cu(III)-oxo and Cu(II)-oxyl. The protonated complexes, however, have nearly pure Cu(III)-character based upon geometric, electronic, and vibrational data.

The relative reactivities of the copper–oxygen complexes toward substrates were addressed by computing their reduction potentials and pK_b values. The 1:1 adducts and Cu(III)-hydroperoxides proved both difficult to reduce and to protonate compared to the Cu(III)-oxo and Cu(III)-hydroxide congeners. This leads to low O—H bond dissociation energies for O—H bonds formed upon hydrogen-atom abstraction from substrates by the 1:1

adducts and Cu(III)-hydroperoxides. Computation of hydrogen-atom abstraction transition-state structures and activation enthalpies for reactions between the various copper–oxygen species and a range of substrates confirmed the low reactivity of the 1:1 adducts and Cu(III)-hydroperoxides and showed that, by contrast, Cu(III)-oxo and Cu(III)-hydroxide species should readily hydroxylate substrates.

Although the electron-rich nature of the β-diketiminate and anilido-imine ligands promotes dioxygen binding, this over-stabilizes 1:1 adducts toward reduction and protonation, and hence reaction with hydrocarbon substrates. The η^1 1:1 Cu-O_2 adducts, while still unreactive, suffer from diminished reactivity to a slightly lesser degree than the corresponding η^2 isomers. These results suggest that new biomimetic model systems for DβM and PHM should employ less electron-donating ligands (e.g., by incorporation of electron-withdrawing groups into the ligand or by using neutral rather than anionic ligands) and be designed to promote end-on *versus* side-on dioxygen binding.

The current data also support the hypothesis that a Cu(II)-superoxide species would be a competent hydroxylating agent in DβM and PHM. Any species with significant Cu(III)-peroxo character will be far slower to react with substrate. The efficacy with which the Cu(III)-oxo species supported by L^1 and L^2 engage in hydrogen-atom abstraction suggests that if such intermediates are formed at the DβM or PHM Cu_B sites, they will be sufficiently strong oxidants to hydroxylate physiological substrates.

Supplementary Material

Tables S1 and S2, Figures S1–S7, and atomic coordinates for each computed geometry.

References

1. Solomon, E. I.; Sundaram, U. M.; Machonkin, T. E. Chem Rev 1996, 96, 2563.
2. Solomon, E. I.; Chen, P.; Metz, M.; Lee, S. K.; Palmer, A. E. Angew Chem Int Ed Engl 2001, 40, 4570.
3. Klinman, J. P. Chem Rev 1996, 96, 2541.
4. Stewart, L. C.; Klinman, J. P. Annu Rev Biochem 1988, 57, 551.
5. Eipper, B. A.; Stoffers, D. A.; Mains, R. E. Annu Rev Neurosci 1992, 15, 57.
6. McMahon, A.; Geertman, R.; Sabban, E. L. J Neurosci Res 1990, 25, 395.
7. Stoffers, D. A.; Green, C. B.; Eipper, B. A. Proc Natl Acad Sci USA 1989, 86, 735.
8. Tian, G. C.; Berry, J. A.; Klinman, J. P. Biochemistry 1994, 33, 226.
9. Evans, J. P.; Ahn, K.; Klinman, J. P. J Biol Chem 2003, 278, 49691.
10. Prigge, S. T.; Kolhekar, A. S.; Eipper, B. A.; Mains, R. E.; Amzel, L. M. Science 1997, 278, 1300.
11. Prigge, S. T.; Kolhekar, A. S.; Eipper, B. A.; Mains, R. E.; Amzel, L. M. Nat Struct Biol 1999, 6, 976.
12. Prigge, S. T.; Eipper, B. A.; Mains, R. E.; Amzel, L. M. Science 2004, 304, 864.
13. Gherman, B. F.; Heppner, D. E.; Tolman, W. B.; Cramer, C. J. J Biol Inorg Chem 2006, 11, 197.
14. Kamachi, T.; Kihara, N.; Shiota, Y.; Yoshizawa, K. Inorg Chem 2005, 44, 4226.
15. Yoshizawa, K.; Kihara, N.; Kamachi, T.; Shiota, Y. Inorg Chem 2006, 45, 3034.
16. Francisco, W. A.; Blackburn, N. J.; Klinman, J. P. Biochemistry 2003, 42, 1813.
17. Chen, P.; Bell, J.; Eipper, B. A.; Solomon, E. I. Biochemistry 2004, 43, 5735.
18. Chen, P.; Solomon, E. I. J Am Chem Soc 2004, 126, 4991.
19. Lewis, E. A.; Tolman, W. B. Chem Rev 2004, 104, 1047.
20. Johansson, A. J.; Blomberg, M. R. A.; Siegbahn, P. E. M. Inorg Chem 2006, 45, 1491.
21. Smirnov, V. V.; Roth, J. P. J Am Chem Soc 2006, 128, 3683.
22. Schatz, M.; Raab, V.; Foxon, S. P.; Brehm, G.; Schneider, S.; Reiher, M.; Holthausen, M. C.; Sundermeyer, J.; Schindler, S. Angew Chem Int Ed Engl 2004, 43, 4360.
23. Cheruzel, L. E.; Cecil, M. R.; Edison, S. E.; Mashuta, M. S.; Baldwin, M. J.; Buchanan, R. M. Inorg Chem 2006, 45, 3191.
24. Blackburn, N. J.; Hasnain, S. S.; Pettingill, T. M.; Strange, R. W. J Biol Chem 1991, 266, 23120.
25. Reedy, B. J.; Blackburn, N. J. J Am Chem Soc 1994, 116, 1924.
26. Boswell, J. S.; Reedy, B. J.; Kulathila, R.; Merkler, D.; Blackburn, N. J. Biochemistry 1996, 35, 12241.
27. Kolhekar, A. S.; Keutmann, H. T.; Mains, R. E.; Quon, A. S. W.; Eipper, B. A. Biochemistry 1997, 36, 10901.
28. Aboelella, N. W.; Kryatov, S. V.; Gherman, B. F.; Brennessel, W. W.; Young, V. G., Jr.; Sarangi, R.; Rybak-Akimova, E. V.; Hodgson, K. O.; Hedman, B.; Solomon, E. I.; Cramer, C. J.; Tolman, W. B. J Am Chem Soc 2004, 126, 16896.
29. Reynolds, A. M.; Gherman, B. F.; Cramer, C. J.; Tolman, W. B. Inorg Chem 2005, 44, 6989.
30. Reynolds, A. M.; Lewis, E. A.; Aboelella, N. W.; Tolman, W. B. Chem Commun 2005, 2014.
31. Schrodinger, LLC. Jaguar 5.0; Schrodinger, LLC, Portland, OR, 2002.
32. Johnson, B. G.; Gill, P. M. W.; Pople, J. A. J Chem Phys 1993, 98, 5612.
33. Becke, A. D. J Chem Phys 1993, 98, 1372.
34. Lee, C. T.; Yang, W. T.; Parr, R. G. Phys Rev B 1988, 37, 785.
35. Ducere, J.-M.; Goursot, A.; Berthomieu, D. J Phys Chem A 2005, 109, 400.
36. Gherman, B. F.; Cramer, C. J. Inorg Chem 2004, 43, 7281.
37. Aboelella, N. W.; Gherman, B. F.; Hill, L. M.; York, J. T.; Holm, N.; Young, V. G., Jr.; Cramer, C. J.; Tolman, W. B. J Am Chem Soc 2006, 128, 3345.
38. Hay, P. J.; Wadt, W. R. J Chem Phys 1985, 82, 270.
39. Wadt, W. R.; Hay, P. J. J Chem Phys 1985, 82, 284.
40. Hay, P. J.; Wadt, W. R. J Chem Phys 1985, 82, 299.
41. Peng, C. Y.; Schlegel, H. B. Isr J Chem 1993, 33, 449.
42. Glendening, E. D.; Badenhoop, J. K.; Reed, A. E.; Carpenter, J. E.; Bohmann, J. A.; Morales, C. M.; Weinhold, F. NBO 5.0.; Theoretical Chemistry Institute, University of Wisconsin, Madison, WI, 2001. http://www.chem.wisc.edu/~nbo5
43. Friesner, R. A.; Baik, M.-H.; Guallar, V.; Gherman, B. F.; Wirstam, M.; Murphy, R. B.; Lippard, S. J Coord Chem Rev 2003, 238/239, 267.
44. Baik, M.-H.; Newcomb, M.; Friesner, R. A.; Lippard, S. J. Chem Rev 2003, 103, 2385.
45. Scott, A. P.; Radom, L. J Phys Chem 1996, 100, 16502.
46. Marten, B.; Kim, K.; Cortis, C.; Friesner, R. A.; Murphy, R. B.; Ringnalda, M. N.; Sitkoff, D.; Honig, B. J Phys Chem 1996, 100, 11775.
47. Tannor, D. J.; Marten, B.; Murphy, R.; Friesner, R. A.; Sitkoff, D.; Nicholls, A.; Ringnalda, M.; Goddard, W. A.; Honig, B. J Am Chem Soc 1994, 116, 11875.
48. Carvajal, C.; Tolle, K. J.; Smid, J.; Szwarc, M. J Am Chem Soc 1965, 87, 5548.

49. Metz, D. J.; Glines, A. J Phys Chem 1967, 71, 1158.
50. Cramer, C. J. Essentials of Computational Chemistry. Theories and Models, 2nd ed.; Wiley: West Sussex, England, 2004.
51. Tissandier, M. D.; Cowen, K. A.; Feng, W. Y.; Gundlach, E.; Cohen, M. H.; Earhart, A. D.; Coe, J. V.; Tuttle, T. R. J Phys Chem A 1998, 102, 7787.
52. Kelly, C. P.; Cramer, C. J.; Truhlar, D. G. J Phys Chem B (in press).
53. Ribas, X.; Jackson, D. A.; Donnadieu, B.; Mahia, J.; Parella, T.; Xifra, R.; Hedman, B.; Hodgson, K. O.; Llobet, A.; Stack, T. D. P. Angew Chem Int Ed Engl 2002, 41, 2991.
54. Winget, P.; Cramer, C. J.; Truhlar, D. G. Theor Chem Accounts 2004, 112, 217.
55. Lide, D. R. Handbook of Chemistry and Physics, 85th ed.; CRC: Boca Raton, 2004.
56. Andersson, K.; Malmqvist, P. A.; Roos, B. O. J Chem Phys 1992, 96, 1218.
57. Karlstrom, G.; Lindh, R.; Malmqvist, P. A.; Roos, B. O.; Ryde, U.; Veryazov, V.; Widmark, P. O.; Cossi, M.; Schimmelpfennig, B.; Neograd y, P.; Seijo, L. Comput Matl Sci 2003, 28, 222.
58. Barandiaran, Z.; Seijo, L. Can J Chem 1992, 70, 409.
59. Pierloot, K.; Dumez, B.; Widmark, P. O.; Roos, B. O. Theor Chim Acta 1995, 90, 87.
60. Binkley, J. S.; Pople, J. A.; Hehre, W. J. J Am Chem Soc 1980, 102, 939.
61. Hehre, W. J.; Stewart, R. F.; Pople, J. A. J Chem Phys 1969, 51, 2657.
62. Mayer, J. M. Comments Inorg Chem 1988, 8, 125.
63. Mayer, J. M. Inorg Chem 1988, 27, 3899.
64. Griffith, W. P. Coord Chem Rev 1970, 5, 459.
65. Kitajima, N.; Koda, T.; Iwata, Y.; Morooka, Y. J Am Chem Soc 1990, 112, 8833.
66. Kitajima, N.; Morooka, Y. Chem Rev 1994, 94, 737.
67. Vaska, L. Accounts Chem Res 1976, 9, 175.
68. Whitham, C. J.; Ozeki, H.; Saito, S. J Chem Phys 2000, 112, 641.
69. Ikeda, S.; Nakajima, T.; Hirao, K. Mol Phys 2003, 101, 105.
70. Mayer, J. M. Accounts Chem Res 1998, 31, 441.
71. Francisco, W. A.; Knapp, M. J.; Blackburn, N. J.; Klinman, J. P. J Am Chem Soc 2002, 124, 8194.
72. Miller, S. M.; Klinman, J. P. Biochemistry 1985, 24, 2114.
73. Freeman, J. C.; Villafranca, J. J.; Merkler, D. J. J Am Chem Soc 1993, 115, 4923.